PRAMANA
— journal of
physics



Vol. 61, No. 5
November 2003
pp. 847–858

# Review of Brookhaven nuclear transparency measurements in ($p$,2$p$) reactions at large $Q^2$

ALAN S CARROLL
Collider-Accelerator Department, Brookhaven National Laboratory, Upton, NY 11973, USA

**Abstract.** In this contribution we summarize the results of two experiments to measure the transparency of nuclei in the $(p,2p)$ quasi-elastic scattering process near 90° in the $pp$ center-of-mass. The incident momenta went from 6 to 14.4 GeV/c, corresponding to $4.8 < Q^2 < 12.7$ (GeV/c)$^2$. First, we describe the measurements with the newer experiment, E850, which has more complete kinematic definition of quasi-elastic events. E850 covers a larger range of incident momenta, and thus provides more information regarding the nature of the unexpected fall in the transparency above 9 GeV/c. Second, we review the techniques used in an earlier experiment, E834, and show that the two experiments are consistent for the carbon data. We use the transparencies measured in the five nuclei from Li to Pb to set limits on the rate of expansion for protons involved in quasi-elastic scattering at large momentum transfer.

**Keywords.** Nuclear; color transparency; protons; alternating gradient synchrotron; large angle.

**PACS Nos 13.85.Dz; 25.40.Cm**

## 1. Introduction

Transparency, $T$, for $(p,2p)$ as illustrated in figure 1 is defined as the ratio of the differential cross-section, integrated over the momentum distribution of the protons in the nucleus, to the differential cross-section for free $pp$ scattering corrected for the number of protons in the nucleus, $Z$.

There have been two major experiments on the transparency of nuclei at the alternating gradient synchrotron (AGS) located at Brookhaven National Laboratory. We use a secondary hadron beam with identification from 6 to 14.4 GeV/c to study the quasi-elastic (q.e.) scattering of protons $(p,2p)$ at angles near 90° in the $pp$ center of mass (CM). A large superconducting solenoid surrounding the target region magnetically analyzes most of the outgoing particles, and provides large acceptance [1,2]. With this detector we are able to extend the energy range of the earlier experiment, E834, in order to investigate the fall in transparency seen above ∼9 GeV/c.

Experiment, E834, utilizes a single high resolution magnetic spectrometer and large solid angle coverage for the recoil particle [3]. We show that the two independent experiments give consistent results for the overlapping carbon data. The extensive data on the transparency of five different nuclei allow a study of the rate of expansion of protons involved in the interaction.

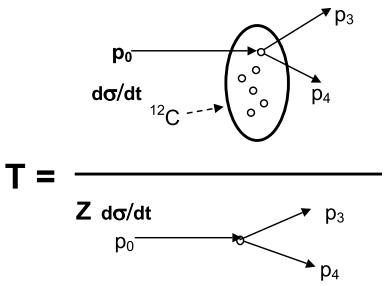


**Figure 1.** Illustration of the quantities used in the determination of transparency.

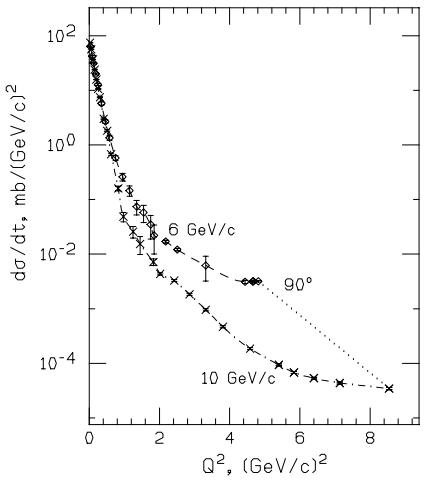


**Figure 2.** $pp$ elastic differential cross-sections for 6 and 10 GeV/c.

## 2. Exclusive reactions at large $p_t$

Transparency can in principle be measured for any exclusive reaction, but the $(p,2p)$ reaction has been chosen because it has a relatively large cross-section at large $p_t$, and proton beams are more intense. Figure 2 shows $pp$ elastic differential cross-section at 6 and 10 GeV/c. In the forward direction the diffractive cross-section is nearly constant with incident energy reflecting the size of the protons. Near 90° CM the behavior changes dramatically. The cross-section becomes nearly flat with CM angle, and the magnitude drops as $s^{-\sim 10}$. The flatness is indicative of possible parton scattering, and the rapid $s$ dependence is ascribed to the short distance of the interaction. A study of a variety of exclusive reactions indicates that the cross-sections at a fixed angle follow a quark counting rule, e.g. [4].

$$\mathrm{d}\sigma/\mathrm{d}t \propto s^{-(n_0+n_2+n_3+n_4-2)}, \tag{1}$$

where $n_0$, $n_2$, $n_3$, and $n_4$ are the number of valence quarks in the hadrons of the initial $(0,2)$ and final $(3,4)$ states.

## 3. Models of transparency

The expected behavior of nuclear transparency at low $Q^2$ is predicted by the Glauber model. As indicated in figure 1, the protons entering and leaving the nucleus are exponentially attenuated by their interaction with the nuclear material. Since the total cross-section is very close to a constant with energy for all the particles associated with interactions in these experiments, the transparency is expected to be constant as well.

Mueller [5] and Brodsky [6] suggested that the transparency would be increased compared to a Glauber calculation whenever the hadrons involved had undergone a q.e. scattering at large momentum transfer. This was because the scaling laws of large angle scattering suggested that the valence quarks in the hadrons were in a point-like configuration (PLC) at the time of interaction. This concept is generally referred to as a color transparency (CT) since the QCD interaction is considerably reduced by the near proximity of the quark color charges in the PLC. Then for high momenta, the hadrons would expand sufficiently slowly over distances compared to nuclear radii to produce an anomalously high transparency compared to that predicted by standard Glauber models. The transparency would approach 1.0 as the momentum was increased.

Two general classes of models have been developed to explain the behavior of hadronic interactions inside a nuclear medium. In the expansion class of models, the high $p_{\mathrm{t}}$ interaction is presumed to select nearly point-like configurations (PLCs) of valence quarks in the interacting protons [5]. These PLCs proceed to expand as their distance increases from the point of interaction.

The second class of models emphasizes that in the nuclear medium, the major effect is to strongly attenuate the large transverse portion of the proton wave function. This nuclear filtering picture is primarily the work of Jain, Ralston, Pire [7–9]. This model suggests that the effective cross-section will be smaller than that of the free cross-sections, and remain essentially constant as it passes through the nucleus. Heppelmann noted early on that the transparencies could be fits with a reduced effective cross-section [10].

The rate of expansion is described in both partonic and hadronic representations [11,12]. Farrar *et al* [11] suggested the expansion parametrization for the effective interaction cross-section, $\sigma_{\mathrm{eff}}(z, Q^2)$ given by eq. (2) [11]. This form is a convenient one for this study:

$$\sigma_{\mathrm{eff}}(z, Q^2) = \sigma_{\mathrm{eff}}^{\infty}\left(\left[\left(\frac{z}{l_h}\right)^{\tau} + \left(\frac{r_t (Q^2)^2}{r_t^2}\right) \times \left(1 - \left(\frac{z}{l_h}\right)^{\tau}\right)\right]\theta(l_h - z) + \theta(z - l_h)\right), \tag{2}$$

where $l_h$ is the expansion distance of the protons and $z$ is the distance from the interaction point. $\sigma_{\mathrm{eff}}(z, Q^2)$ expands linearly or quadratically from its initial size depending on the value of $\tau$, and then assumes the free space value, $\sigma_{\mathrm{eff}}^{\infty}$, when $z = l_h$. As noted below, the actual value of $\sigma_{\mathrm{eff}}^{\infty}$ used in the fitting procedure may be less than the free $\sigma_{\mathrm{tot}}(pN)$ for the proton–nucleon interaction because a portion of the q.e. events with an initial or final state elastic scattering fall within the kinematical definition of a q.e. event. Since all the measurements are made near 90° CM, numerically $Q^2 \simeq p_0$. For convenience of calculation, in this paper an expansion parameter, $\lambda$, scaled to 6 GeV/c has been used to parametrize all the proton momenta in the interaction. That is, the expansion distance $l_h$ for each leg of the calculation shown in figure 1 is given by $l_h = \lambda(p_f/6)$ fm.

The exponent $\tau$ allows for three suggested pictures of expansion; $\tau = 0$, 1, and 2. For $\tau$ = 1, the expansion corresponds to the 'quantum diffusion' picture [11]. For this picture, $l_h = 2p_f/\Delta(M^2)$ where $p_f$ is the momentum of a proton traveling through the nucleus and $\Delta(M^2)$ is the mass difference of an intermediate state [11]. The authors of [11] indicate the values of $\Delta(M^2)$ between 0.5 and 1.1 GeV$^2$ are acceptable corresponding to values of $l_h = 0.36p_f$ to $0.78p_f$ fm, or $2.1 < \lambda < 4.6$ fm.

The case of $\tau = 2$ is generally referred to as the naive quark expansion scenario in which the light quarks fly apart at a maximum rate and the distance is determined by the Lorentz boost to the hadrons. In this case $l_h \simeq E/m_h$, so for protons at 6 GeV/c, $\lambda$ equals $\sim 7.3$ fm [11]. The quantity $\langle r_t(Q^2)^2\rangle / \langle r_t^2\rangle$ represents the fraction of $\sigma_{\text{eff}}$ at the time of interaction.

Given that the initial and final states in these $(p, 2p)$ q.e. interactions are exclusive hadrons, the approach of Jennings and Miller to represent the proton expansion in terms of a set of hadronic states seems very reasonable [12,13]. This representation explicitly notes that a PLC cannot be a simple proton, but must include a superposition of excited states. In their model, $\lambda = 0.9$ fm for $\tau = 1$, and $\lambda = 2.4$ fm for $\tau = 2$.

Because in the nuclear filtering picture, the long distance portion of the amplitude is filtered away by the nuclear medium, the cross-section for q.e. scattering in the nucleus will follow the scaling behavior, whereas the unfiltered free $pp$ cross-section will show oscillations about the $s^{-10}$ scaling. Thus the variations in the nuclear transparency are mainly due to the oscillations in the free $pp$ cross-section about the cross-section with exact scaling. In fitting the transparency, no expansion should be required, only a smaller effective cross-section. In this model of the second class, $\tau$ is set to 0 and so eq. (2) reduces to, $\sigma_{\text{eff}}(z, Q^2) = \sigma_{\text{eff}}(Q^2)$ [14].

## 4. E850 Experiment

The E850 experiment embeds the nuclear and $CH_2$ targets inside a 2 m diameter, 3 m long 0.8 T superconducting solenoid as shown in figure 3. Surrounding the targets were four concentric cylinders (C1–C4) of mean radii: 10, 45, 90, and 180 cm. Each cylinder was made up of four layers of straw tubes of 0.50, 1.04, 1.04, and 2.16 cm diameter.

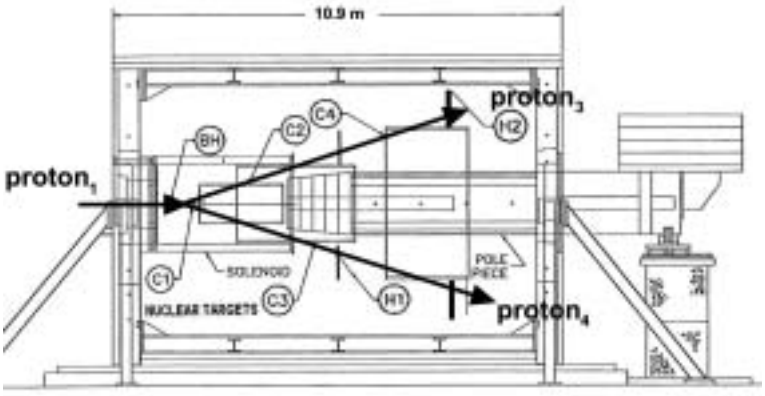


**Figure 3.** Schematic drawing of E850 solenoidal detector with incident proton$_1$ and outgoing proton$_3$ and proton$_4$.

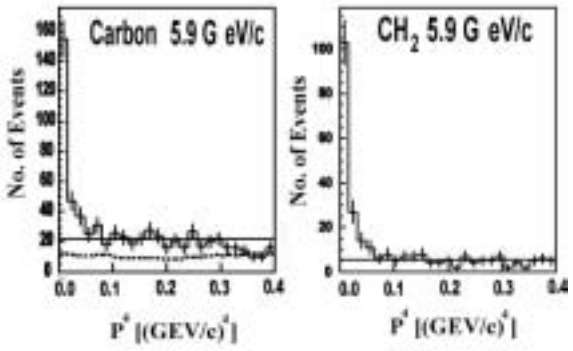


**Figure 4.** $P^4$ distribution for 5.9 GeV/c. The dotted line in the left hand plot shows the events with an additional track.

The tracks scattered near 90° CM pass through the annulus between the solenoid and the steel pole piece until they reached the scintillation counters and the largest straw tube cylinder. The trigger system selects only events with particles above a minimum $p_t$ [15].

After track reconstruction we could calculate the vertex, and the four momenta of each track under the assumption that it was a proton. Then by subtraction the four momenta, $p_f$, of the target protons are calculated. The analysis combines these quantities into one variable, $P^4$, related to four-dimensional volume element of target proton [2]. As seen in figure 4, there is a clear peak at small values of $P^4$, and flat distribution beyond that. Selecting events with an additional track in the innermost cylinder, the upper plot shows a flat distribution (dotted line) in $P^4$ which extends under the peak.

## 5. E834 Experiment

The E834 detector was originally built for the measurements of a large number of two-body exclusive reactions at $\sim$90° CM with a liquid hydrogen target [4]. The location of the experiment and the beam line is the same as that used for E850. One long-lived particle was detected with a high resolution magnetic spectrometer ($\Delta p/p = 1\%$) which determines both its direction and momentum. Then a very large acceptance array of wire chambers measures the directions of any conjugate particles which are elastically scattered, results from a resonance decay, or nearly all of the q.e. distribution at one setting.

The target array consists of two $CH_2$ blocks on either end of the 4 targets of either Li, C, Al, Cu, or Pb as indicated by the vertex distribution in figure 5. Two sandwiches of lead and scintillator above and below the targets detected charged particles or gammas in addition to the two measured protons from a q.e. scattering.

Since there was a momentum measurement of only one of the two final state particles, q.e. reactions are in principle lacking one constraint. However, the binding energy and Fermi momentum of the struck proton are small compared to the momenta of the incident and final state particles so that neglecting these terms in the energy balance is a small (0.5%) effect.

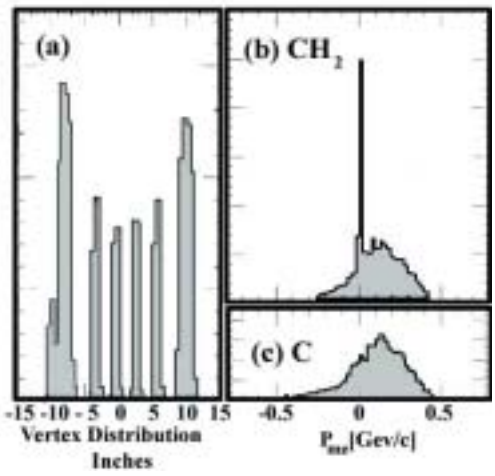


**Figure 5.** Some of the quantities measured in E834 experiment; the vertex position (**a**), and the $p_z(p_{mz})$ distribution for the $CH_2$ (**b**) and C (**c**) targets.

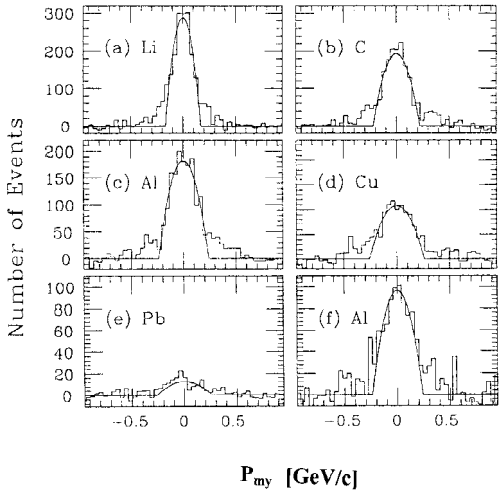


**Figure 6.** The out-of-plane $p_y(p_{my})$ distributions for Li, C, Al, Cu and Pb targets with backgrounds subtracted. The fitted curves are derived from electron scattering.

The out-of-plane Fermi component, $p_{fy}$, is determined to be $\pm 30$ MeV/c, the longitudinal component, $p_{fz}$ to be $\pm 10$ MeV/c, while the transverse in-plane component, $p_{fx}$, is known to be only about $\pm 100$ MeV/c. Some of the measured quantities are shown in figure 5. The distribution of the $p_{fz}$ component readily allows the H component of the $CH_2$ target to be seen as in figure 5.

The transverse components have a negligible effect on center of mass energy *s*, and $p_y$ is the better determined component. So we plot the number of events vs. $p_y$ as shown in figure 6 for carbon and lead. The events appearing in this plot have been selected in

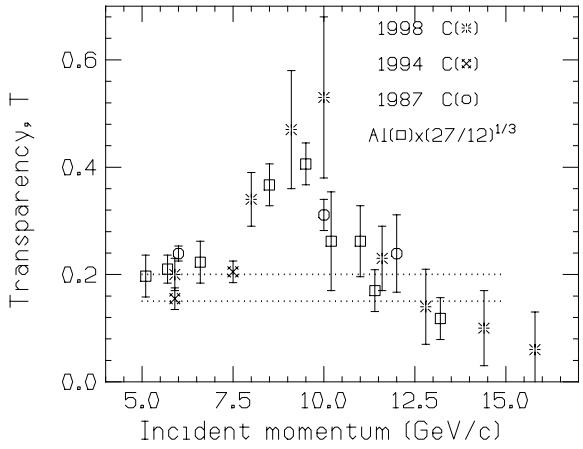


**Figure 7.** Summary of transparency measurements from E850 and E834. The dotted lines indicate the range of Glauber calculations.

$0.2 < p_{fz} < -0.1$, and have $\|p_{fx}\| < 0.25$ GeV/c. The background determined from events with $>1$ hits in the veto planes is subtracted in these distributions [3].

## 6. Energy dependence of transparency

A series of measurements made at the AGS have determined nuclear transparencies for a number of different momenta and nuclei. The carbon transparencies as a function of incident momentum for the 1998 data from E850 by Leksanov *et al* [2] and the 1994 data from E850 by Mardor *et al* [1], and the 1987 data from E834 by Carroll *et al* [3] are shown in figure 7. Also included are the 1987 Al data from E834 which has been scaled as $(27/12)^{1/3}$, the ratio of the Al to C nuclear radii to indicate the consistency of these two nuclei.

These measurements of $(p, 2p)$ q.e. scattering in nuclei indicate effective cross-sections for absorption in nuclei, which vary with incident momenta from 6 to 14.4 GeV/c, and are in general significantly less than the measured *pN* total cross-sections. All measurements consistently show a rise to 9 GeV/c, then fall back to the 6 GeV/c levels or below. The dotted lines show the carbon transparencies calculated with the Glauber method for $\sigma_{\text{eff}}$ between 36 and 40 mb by a number of authors [16–18].

## 7. A dependent analysis

This *A* dependent analysis is the work of the speaker, and does not necessarily reflect the consensus of the collaboration [19].

The expected transparencies are calculated by the Monte Carlo method as a function of incident momentum ($p_0$), nucleus (A), effective cross-section ($\sigma_{\text{eff}}$), and expansion distance ($\lambda$) at a number of closely spaced values. Then these calculated transparencies are used to find the best fit to the experimentally measured values.

The integrals for calculating the transparency at each incident momentum, $p_0$, and outgoing momenta, $p_3$ and $p_4$, are given by the following expressions. This transparency is given by, $T(\sigma_{\rm eff}, A, \lambda) = r_n(p_0)P_0P_3P_4$, where the $P_i$ are the average survival probabilities of the protons on each of the three legs as shown in figure 1. $r_n(p_0)$ is a normalization parameter included to allow for normalization uncertainties in both the data and the phenomenology. The integrals (eq. (3)), along each of the three paths in $z$ are from the randomly selected interaction points to the edge of the nucleus.

$$P_i = \exp\left[-\int_{\rm path} {\rm d}z' \sigma_{\rm eff}(p_i, z, \lambda_i)\rho_A(r_i)\right]. \tag{3}$$

A Woods–Saxon form was used for the density, $\rho_A(r_i) = c/(1+\exp(-R+r_i/b))$, where $r_i$ is the radial distance from the nucleus center to a point along the $i$th path. The parameter $b$ is set to 0.56 fm, and then the $\langle$rms$\rangle$ radii are matched to electron scattering results [20]. The integrated density is equal to the $A$ of the nucleus. The effect of correlations on the calculated transparencies is studied and found to be small [18,19]. The transparency was calculated for five different nuclear targets at each momentum in fine steps $\sigma_{\rm eff}$ and $\lambda$.

Using the generated values of the transparency, a best fit was made to the values for 6, 10, and 12 GeV/c (or 6 and 10 GeV/c only). The search determined the best fit by minimizing the $\chi^2$ function to the 12 (or 10) transparencies as given in eq. (4).

$$\chi^2 = \Sigma_{k=1}^{3}(\Sigma_{i=1}^{5}([(r_n(p_{0,k})T_{i,k}({\rm fit}) - T_{i,k}({\rm meas}))/(\Delta T_{i,k}({\rm meas}))]^2)), \tag{4}$$

where there are sums for the momenta ($k$), (6, 10, and 12 GeV/c) and the 5 nuclei ($i$) (2 nuclei at 12 GeV/c). To fit with the nuclear filtering model the exponent, $\tau$, is set to 0, and $\sigma_{\rm eff}$ is allowed to vary from 1 to 45 mb at each $p_0$.

Figure 8 gives the result of fitting the transparencies to the linear ($\tau = 1$) expansion hypothesis. The values of $\sigma_{\rm eff}$ are constrained to be greater than 32 mb, and equal in magnitude at each step in $\lambda$. The values of $r_n(p_{0,k})$ are held to be within $\pm$15% of each other at each step. The solid curve starting at $\sim$60 corresponds to minimizing the $\chi^2$ parameter in the fit to the 6, 10, and 12 GeV/c transparencies. The minimum value of this $\chi^2$ curve is 19 which has a probability of 1.5%.

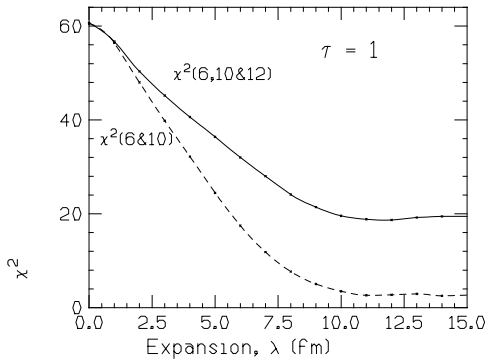


**Figure 8.** The $\chi^2$ and fitted parameters for a fit to transparencies with linear expansion model, $\tau = 1$ for both 6, 10, and 12 GeV/c, and for 6 and 10 GeV/c alone.

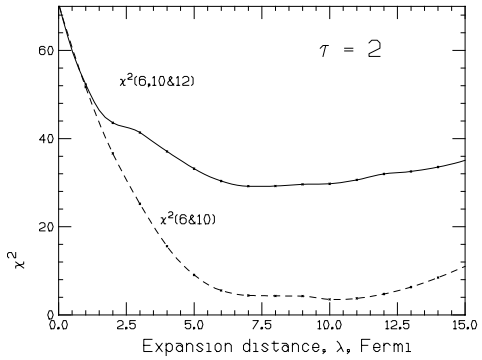


**Figure 9.** Fit to transparencies with quadratic expansion model ($\tau = 2$). The meaning of the curves is the same as for the $\tau = 1$ case.

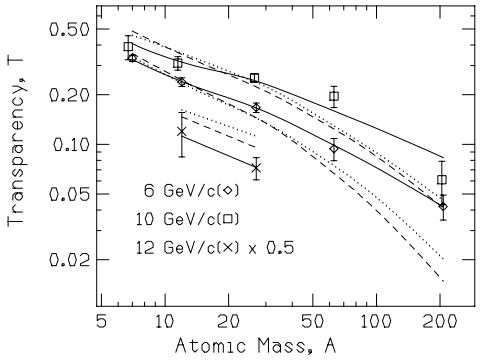


**Figure 10.** Representative fits to transparencies. The nuclear filtering model $\tau = 0$ is represented by the solid curves, and the $\tau = 1$ and $\tau = 2$ expansion models at $\lambda = 3$ fm are displayed as the dashed and dotted curves respectively. Note that the 12 GeV/c transparencies have been multiplied by 0.5 to avoid overlap with the 6 GeV/c results.

The dashed curve in figure 8 starting at ∼60 is the $\chi^2$ for fitting only the 6 and 10 GeV/c transparencies. The probability of $\chi^2$ reaches 5% for values of $\lambda > 6.4$ fm.

The results of fitting to the quadratic expansion ($\tau = 2$) are shown in figure 9. $\chi^2$ for the fit to the 6, 10, and 12 GeV/c transparencies (solid curve) never goes below 29.2, corresponding to a probability of less than 0.012. For the case of a fit to only the 6 and 10 GeV/c data (dashed curve), the probability reaches 5% at $\lambda = 4.0$ fm.

The $\tau = 0$ column of table 1 displays the values of a fit with nuclear filtering ($\tau = 0$). Here the values of $\sigma_{\text{eff}}$ are allowed to vary independently at each momentum without constraints on the value of $\sigma_{\text{eff}}$. The errors are determined from the one standard deviation in the ln(Likelihood) [21]. Jain and Ralston found values of $17 \pm 2$ mb and $12 \pm 2$ mb for $\sigma_{\text{eff}}$ (6 GeV/c) and $\sigma_{\text{eff}}$ (10 GeV/c) which are consistent with this analysis [14].

Figure 10 illustrates the quality of the fit to the experimentally measured transparencies for each of the five nuclei at 6, 10, and 12 GeV/c for the three models; namely for $\tau = 0$ for

the nuclear filtering model, and $\lambda = 3$ fm for $\tau = 1$ and $\tau = 2$. At this expansion distance, the $\tau = 1$ and $\tau = 2$ expansion models indicate a fall-off of transparency with $A$ which is much steeper than that measured. Generally reasonable fits can be made with the $\tau = 1$ and $\tau = 2$ expansion models to the 6 and 10 GeV/c transparencies alone when $\lambda$ is greater than 6 fm. However, only the nuclear filtering (solid curve) can simultaneously fit to the 6, 10, and 12 GeV/c transparencies.

## 8. Summary

Two independent experiments show the same unexpected momentum dependence for $(p,2p)$ transparency at large $Q^2$. For $(e,e'p)$ experiments for $Q^2$ up to 9 (GeV/c)$^2$, there is no indication of momentum dependence in transparency [22]. Apparently, the variation of the $(p,2p)$ transparencies is due to the more complex nature of the $(p,2p)$ amplitudes.

Table 1 presents a summary of the $A$ dependent analysis, and predictions of various models. Due to the oscillatory nature of the $(p,2p)$ transparency with incident momentum, it is not surprising that no acceptable fit with Prob$(\chi^2) > 0.05$ can be achieved with a simple, unified expansion model simultaneously fitting to the data at 6, 10, and 12 GeV/c. As has been noted by various authors, additional amplitudes are needed to account for the sudden drop in transparency between 10 and 12 GeV/c. This measured drop in the transparency has been verified by the E850 experiment, and is shown in figure 7 to continue to higher momenta [2].

For Ralston and Pire, the drop in transparency is connected with the interference of the short distance pQCD amplitude with that of the long distance Landshoff contribution [7]. Brodsky and de Teramond [23] noted the strong correlation in energy between the striking spin dependence of $pp$ scattering [24] and the behavior of the $(p,2p)$ transparency [3]. They suggested that the drop in transparency at 12 GeV/c could be due to the presence of a resonance in the $pp$ channel due to the threshold for charm particles which creates a long-range amplitude.

**Table 1.** Summary of fit parameters and comparison to models.

| This Analysis<br>Momenta Fit | $\tau = 0$<br>6,10, and 12 | $\tau = 1$<br>6 and 10 | $\tau = 1$<br>6,10, and 12 | $\tau = 2$<br>6 and 10 | $\tau = 2$<br>6,10, and 12 |
|---|---|---|---|---|---|
| Prob$(\chi^2)$ | 0.87<br>const. | $> 0.05$<br>for | $< 0.044$<br>for | $> 0.05$<br>for | $< 0.012$<br>for |
| $\lambda$ (fm) | | $> 6.4$ | all | $> 4.0$ | all |
| $\sigma_{\text{eff}}$ (6 GeV/c) (mb) | $17.9^{+2.7}_{-1.5}$ | | | | |
| $\sigma_{\text{eff}}$ (10 GeV/c) (mb) | $12.3^{+2.6}_{-2.6}$ | | | | |
| Farrar *et al* | | | | | |
| Prob$(\chi^2)$ | | $1\times10^{-7}$–$8\times10^{-4}$ | $3\times10^{-7}$–$5\times10^{-5}$ | 0.82 | $1\times10^{-3}$ |
| $\lambda$ (fm) | | 2.1–4.7 | 2.1–4.7 | 7.3 | 7.3 |
| Jennings–Miller | | | | | |
| Prob$(\chi^2)$ | | $2\times10^{-9}$ | $1\times10^{-8}$ | $1\times10^{-4}$ | $6\times10^{-6}$ |
| $\lambda$ (fm) | | 0.9 | 0.9 | 2.4 | 2.4 |

One might imagine that the 6 and 10 GeV/c transparencies represent a simpler set of data where only one set of amplitudes dominate. The maximum expected value of $\lambda$ for the linear ($\tau = 1$) expansion corresponds to an intermediate mass, $\Delta(M^2) = 0.5$ GeV$^2$, corresponding to $\lambda = 4.7$ fm at at 6 GeV/c [11]. At this value Prob($\chi^2$) is $8 \times 10^{-4}$. The hadronic model suggests that $\lambda = 0.9$ fm [12,13]. Thus no linear expansion pictures in either the partonic or the hadronic representations provide expansions long enough to fit the data.

For the $\tau = 2$ expansion, an acceptable fit to 6 and 10 GeV/c is reached at a smaller value of $\lambda$ due to the more rapid fall-off of $\sigma_{\text{eff}}$ with $\lambda$ (see figure 7). Surprisingly, the quadratic expansion ($\lambda \cong 7.3$ fm) in the naive quark picture can provide an acceptable fit to the 6 and 10 GeV/c data. The theoretical basis for such simple behavior seems weak, but it confirms the need for a small $\sigma_{\text{eff}}$.

The nuclear filtering picture provides an acceptable representation of the transparencies. There is a different constant value of $\sigma_{\text{eff}}$ for each incident momentum, and hence $Q^2$. However, $\sigma_{\text{eff}}$ shows no expansion over a range of nuclear radii from Li (2.1 fm) to Pb (6.6 fm) and provides an acceptable description of the data as has been shown in previous publications [10,25].

For future $(p, 2p)$ transparency experiments it would be very interesting to extend the momentum range to $\sim$30 GeV/c to see if the oscillations continue. Also a determination of the $A$ dependence for an incident momentum in the range of 12 to 14 GeV/c where the transparency is at a minimum would be important. According to the Jain and Ralston picture [25], the value of $\sigma_{\text{eff}}$ should continue to decrease even though the transparency has fallen by about of factor of two from its carbon value at 9 GeV/c.

## Acknowledgements

It is a pleasure to acknowledge the dedicated efforts of D S Barton, G Bunce, S Gushue, Y I Makdisi, S Heppelmann, H Courant, G Fang, K J Heller, M L Marshak, M A Shupe, J J Russell of the E834 Collaboration and H Aclander, J Alster, G Asryan, V Bauturin, Y Averiche, D S Barton, N Buktoyarova, G Bunce, N Christensen, H Courant, S Durrant, K Gabriel, S Gushue, S Heppelmann, T Kawabata, I Kosonovsky, A Leksanov, Y I Makdisi, A Malki, I Mardor, Y Mardor, M L Marshak, D Martel, E Minima, E Minor, I Navon, H Nicholson, A Ogawa, Y Panebratsev, E Piasetzky, T Roser, J Russell, A Schetkovsky, S Shimanskiy, S Sutton, M Tanaka, A Tang, I Tsetkov, H Yoshida, J Watson, C White, J-Y Wu, D Zhalov of the E850 Collaboration. This work was supported by grants from the US DOE (DEFG0290ER40553), NSF (PHY-9804015), and the US-Israel BSF.

## References

[1] I Mardor *et al*, *Phys. Rev. Lett.* **81**, 5085 (1998)
[2] A Leksanov *et al*, *Phys. Rev. Lett.* **87**, 212301–1 (2001)
[3] A S Carroll *et al*, *Phys. Rev. Lett.* **61**, 1698 (1988)
[4] C White *et al*, *Phys. Rev.* **D49**, 58 (1994)
[5] A Mueller, *Proceedings of the XVII Recontre de Moriond* edited by J Tran Thanh Van (Editions Frontieres, Gif-sur-Yvette, France, 1982)

[6] S J Brodsky, *Proceedings of the XIII International Symposium on Multi-particle Dynamics* edited by W Kittel, W Metzer and A Stergiou (World Scientific, Singapore, 1982)
[7] J P Ralston and B Pire, *Phys. Rev. Lett.* **61**, 1823 (1988)
[8] P Jain, B Pire and J P Ralston, *Phys. Rep.* **271**, 67 (1996)
[9] J P Ralston and B Pire, *Phys. Rev. Lett.(Comment)* **67**, 2112 (1991)
[10] S Heppelmann, *Nucl. Phys. (Proc. Suppl.)* **B12**, 159 (1990)
[11] G R Farrar, H Liu, L L Frankfurt and M I Strikman, *Phys. Rev. Lett.* **61**, 686 (1988)
[12] B K Jennings and G A Miller, *Phys. Rev. Lett.* **69**, 3619 (1992)
[13] B K Jennings and G A Miller, *Phys. Lett.* **B318**, 7 (1993)
[14] P K Jain and J P Ralston, *Phys. Rev.* **D48**, 1104 (1993)
[15] J-Y Wu *et al*, *Nucl. Instrum. Methods Phys.* **A349**, 183 (1994)
[16] L L Frankfurt, M I Strikman and M B Zhalov, *Phys. Rev.* **C50**, 2189 (1994)
[17] L L Frankfurt, M I Strikman and M B Zhalov, *Phys. Lett.* **B503**, 73 (2001)
[18] T-S H Lee and G A Miller, *Phys. Rev.* **C45**, 1863 (1992)
[19] A S Carroll, arXiv:hep-ph/0209288
[20] H De Vries, C W de Jager and C De Vries, *At. Data Nucl. Data Tables* **36**, 495 (1987)
[21] Particle Data Group, *Phys. Rev.* **D54**, 160 (1996)
[22] K Garrow *et al*, *Phys. Rev.* **C66**, 044613 (2002) and references therein
[23] S J Brodsky and G de Teramond, *Phys. Rev. Lett.* **60**, 1924 (1988)
[24] E A Crosbie *et al*, *Phys. Rev.* **D23**, 600 (1981)
[25] P Jain and John P Ralston, *Phys. Rev.* **D46**, 3807 (1992)
[26] L L Frankfurt, E J Moniz, M M Sargsyan and M I Strikman, *Phys. Rev.* **C51**, 3435 (1995)